PERGAMON

Radiation Physics and Chemistry 62 (2001) 301–310

Radiation Physics and Chemistry

www.elsevier.com/locate/radphyschem

Updated NIEL calculations for estimating the damage induced by particles and γ-rays in Si and GaAs

A. Akkerman[a], J. Barak[a,*], M.B. Chadwick[b], J. Levinson[a], M. Murat[a], Y. Lifshitz[a]

[a] *Soreq NRC, Yavne 81800, Israel*
[b] *LANL, Los Alamos, NM 87545, USA*

Received 26 June 2000; accepted 30 January 2001

Abstract

Systematic calculations of the non-ionizing energy losses (NIEL) have been performed for electrons, protons, neutrons and γ-rays in Si and GaAs for a wide range of particle energies. Well-established theoretical approaches as well as newly-developed data (ENDF/B-VI for protons and neutrons) have been used for calculating the differential cross sections for energy transfer to the recoils which in turn produce displacement damage. Some differences, found between our calculations and other works, have been explained. Equivalent fluences of particles, i.e. those introducing the same displacement damage, have been estimated. The updated calculations and models presented here are useful for assessing device performance in space and laboratory tests.

Keywords: Non-ionizing energy loss; Space radiation; Elastic and inelastic interactions

1. Introduction

Many studies over the last decade have shown that device-malfunctioning may occur not only as a result of the ionization induced by charged particles in the device, but also by the damage created by recoils resulting from non-ionizing energy transfer to the semiconductor-lattice atoms. These effects are termed 'non-ionizing energy losses' (NIEL) by the community of 'radiation in space' (though the non-ionizing losses, in particular for low energy particles, also include atomic excitations which do not end up in lattice damage). The NIEL are due to the elastic scattering of the primaries (electrons, protons, α particles, neutrons) as well as of the fragments created in nuclear reactions (inelastic nuclear scattering) of the incident protons or neutrons with the device nuclei. The issue has become important with the extensive use in space programs of LEDs, optocouplers, CCDs etc. Though the problem of calculating the NIEL was in general solved decades ago for solar-cell applications in low space orbits, the need for new insights into NIEL processes, for the use of the above devices in space, has become clear.

Dale et al. (1989a) have shown that it would be convenient to use, for the displacement damage estimation, a quantity named NIEL which gives the portion of energy lost by a particle which leads to displacement damage. It is defined similarly to the linear energy transfer (LET) with units $MeVcm^2/g$. NIEL might be used for estimating the displacement damage effects simultaneously with the LET for estimating total ionizing dose (TID) effects. The subject was recently reviewed by Marshall and Marshall (1999).

The NIEL parameter might be used also for establishing the relations between the displacement effects of different particles and γ-rays or of the same particle with different energies. The resulting equivalence ratio is important for simulating the damage in devices in space

*Corresponding author. Tel.: +972-89434482; fax: +972-8-9434403.

E-mail address: barak@ndc.soreq.gov.il (J. Barak).

0969-806X/01/$ - see front matter
PII: S0969-806X(01)00207-9

by performing measurements in the laboratory. For the displacement damage caused by nuclear particle (protons, neutrons) induced secondaries, it is difficult to obtain the NIEL directly from the experiment, because of the short range of the recoils. The main approach is thus to use theoretical calculations. Such calculations have been performed by several authors in the frame of various theoretical models of nuclear interaction of protons and neutrons with the device-material nuclei (Messenger et al., 1999, and references therein).

Here, we are presenting new calculations of NIEL for electrons, γ-rays, protons and neutrons. The energies of the protons and neutrons are up to 200 MeV, a range which covers most practical energies of these particles in space and laboratory. We have used the most recent data bases of the differential cross sections of the particle interactions in solids, along with the theoretical approaches most appropriate for using these data. In the case of protons and neutrons, this was the extended version of the Evaluated Nuclear Data Files, ENDF/B-VI (Chadwick et al., 1999a), which had been recently used for calculating proton and neutron induced SEU cross sections with reasonably good agreement with experimental SEU results (Chadwick and Normand, 1999).

Systematic comparison of our results with existing theoretical estimations of the NIEL and with experimental data has shown good agreement in most cases, thereby confirming the models and data used in our calculations. Hence, the results presented here can be used for predicting the amount of displacement damages in various devices and for finding equivalent damaging radiation for laboratory tests.

2. General formulation

In this section we derive the expressions to calculate the NIEL for a given primary particle (with an energy T_0) interacting with the lattice atoms (with atomic mass A in atomic mass units, amu) to emit a spectrum of recoils (with atomic mass A_1 in amu and energies T in MeV) which in turn cause displacement damage. The NIEL parameter is defined as the portion of T_0 per unit travelling length (expressed in mass per area) which turns into displacement damage. In the inelastic scattering we have to take into account the partial cross section for each potential recoil particle, from α particles to the lattice atoms (examples see in Table 1). Denoting by $Q(T)$ the partition factor which gives the fraction of T to be lost to NIEL and by $\mathrm{d}\sigma/\mathrm{d}T$ the differential partial cross section for creating a given recoil with energy T, the NIEL is given by

$$\mathrm{NIEL}(T_0) = \frac{N_\mathrm{A}}{A}\int_{T_\mathrm{min}}^{T_\mathrm{max}} \mathrm{d}T\, Q(T) T \left(\frac{\mathrm{d}\sigma}{\mathrm{d}T}\right)_{T_0}, \quad (1)$$

where $N_\mathrm{A} = 6.022 \times 10^{23}$ (Avogadro's number) and $T_\mathrm{max} = 4T_0AA_1/(A+A_1)^2$. We assume that the minimum energy transfer is $T_\mathrm{min} = 2T_\mathrm{d}$ where T_d is the displacement energy. For T_d we use $T_\mathrm{d}(\mathrm{silicon}) = 21\,\mathrm{eV}$ and $T_\mathrm{d}(\mathrm{GaAs}) = 10\,\mathrm{eV}$.

Unlike SEUs, which depend also on the recoil emitting angle θ, the NIEL results from accumulating displacement damage of many recoils and thus does not depend explicitly on θ.

Eq. (1) is written separately for each recoil kind. The total $\mathrm{NIEL}(T_0)$ is found by summing (1) on all these possible recoils.

In *elastic scattering* the recoil is the lattice atom. Since here its energy T is a function of θ we may rewrite Eq. (1) as

$$\mathrm{NIEL}(T_0) = \frac{N_\mathrm{A}}{A}\int_{\theta_\mathrm{min}}^{180^\circ} \mathrm{d}\Omega\, Q[T(T_0,\,\theta)]\, T(T_0,\,\theta)\left(\frac{\mathrm{d}\sigma}{\mathrm{d}\Omega}\right)_{T_0}, \quad (2)$$

where Ω is the solid angle of scattering. From the two body kinematics T depends on the center of mass (CM) scattering angle θ through

$$T(T_0,\,\theta) = T_\mathrm{max}\sin^2(\theta/2) \quad (3)$$

The value of θ_min is obtained from Eq. (3) using $T(T_0,\,\theta_\mathrm{min}) = 2T_\mathrm{d}$.

3. Estimation of the partition factor $Q(T)$

The most complete way to calculate $Q(T)$ is by solving the transport problem of a recoil in matter and estimating all the energy losses along the particle track via elastic or inelastic collisions. This was first done by Lindhard et al. (1963) using an approximate transport

Table 1
Comparison of (a) our calculations with (b) those of Chadwick et al. (1999a) of the relative distribution of fragments of atomic number Z for the inelastic interaction of protons in Si. It is given for two energies: 100 and 150 MeV

E_p (MeV)	$Z=14$		13		12		11		9, 10		7, 8		5, 6	
	(a)	(b)	(a)	(b)	(a)	(b)	(a)	(b)	(a)	(b)	(a)	(b)	(a)	(b)
100	0.17	0.17	0.31	0.27	0.25	0.24	0.11	0.12	0.09	0.14	0.04	0.04	0.01	—
150	0.15	0.16	0.29	0.27	0.19	0.23	0.18	0.09	0.12	0.16	0.06	0.07	0.02	—

kinetic equation. In Lindhard's work the elastic losses have been calculated for the Thomas–Fermi potential, used to describe the energy transfer. Now it is known that this potential overestimates the elastic losses. A more appropriate calculation would be to use a 'softer' potential, such as the 'universal potential' (O'Connor and Biersack, 1986), along with a Monte Carlo transport code such as SRIM (Ziegler et al., 1985).[1] Unfortunately such calculations have not been done. Hence Lindhard's approach, which enables the calculations of Q for various combinations of the primary particle (or recoil) and target atoms, remains the most useful for estimating Q.

According to Lindhard's approach and following Robinson (1968) Q might be expressed by

$$Q = 1/[1 + k_L\, g(\varepsilon)], \tag{4}$$

where ε is Lindhard dimensionless energy. k_L is given by

$$k_L = 0.0794 \frac{Z^{2/3} Z_1^{1/2} (A + A_1)^{3/2}}{(Z^{2/3} + Z_1^{2/3})^{3/4} A^{3/2} A_1^{1/2}}. \tag{5}$$

Z and Z_1 are the atomic numbers and A and A_1—the atomic masses in amu of the lattice atom and the recoil, respectively. $g(\varepsilon)$ is given by

$$g(\varepsilon) = \varepsilon + 0.40244\, \varepsilon^{3/4} + 3.4008\, \varepsilon^{1/6}. \tag{6}$$

4. NIEL for electrons

The elastic cross section $d\sigma/d\Omega$ is given, in the relativistic case, by Mott's formula (Mott and Massey, 1965) which expresses the cross section for a bare nucleus by an infinite converging series. To avoid the computational problems of such a series, approximate formulae have been presented by several authors (see Motz et al., 1964, and references therein). However, these approximations might not be precise enough. Recent calculations have led to a good fitting formula for the Mott differential cross section, $(d\sigma/d\Omega)_M$ (Lijian et al., 1995). It is given by

$$(d\sigma/d\Omega)_M = (d\sigma/d\Omega)_R \sum_{j=0}^{4} a_j(T_0, Z)\,(1 - \cos\theta)^{j/2}, \tag{7}$$

where $(d\sigma/d\Omega)_R$ is the Rutherford cross section which, for the relativistic case, can be written as

$$(d\sigma/d\Omega)_R = \frac{r_0^2 Z^2 (1 - \beta^2)}{\beta^4 (1 - \cos\theta)^2}, \tag{8}$$

where $r_0 = 2.818 \times 10^{-13}$ cm is the classical electron radius and β is the electron velocity in c units. The fitting coefficients a_j can be calculated, for all the elements (all Z's) of the periodic table, using the formulae given by Lijian et al. (1995).

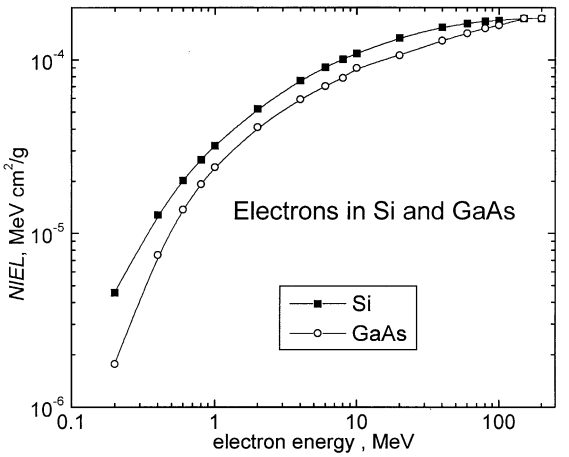

Fig. 1. Electron-NIEL in Si and GaAs versus electron energy. The (spline) line is a guide to the eye.

The last step is to introduce the screening effect of the scattering-atom electrons. This is done here, according to the procedure described by Akkerman (1991), by replacing $(1 - \cos\theta)$ in formulae (7) and (8) by $(1 - \cos\theta + 2\eta)$ with the parameter η calculated according to Nigam et al. (1959). A direct approach for calculating $(d\sigma/d\Omega)$ in a screened potential field was proposed by Berger et al. (1993), yet for 1 MeV electrons we got an excellent agreement with the tabulated $(d\sigma/d\Omega)$ by Berger et al. (1993), obtained using an improved version of the algorithm of Bunyan and Schonfelder (1965) to take into account the screening. For electrons the maximal energy transfer T_{max} is calculated by

$$T_{max} = \frac{2T_0(T_0 + 1.022)}{M_0 c^2 A} \tag{9}$$

where T_0 is the electron kinetic energy in MeV, A—the atomic mass in amu of the lattice-atom and $M_0c^2 = 931.5$ MeV is the equivalent energy for 1 amu. In Fig. 1 we present the results of electron-NIEL for Si and GaAs as a function of the electron energy. Our results are in close agreement with the data calculated by Summers et al. (1993).

The method used for monoenergetic electrons might be easily extended to a given spectrum of electrons in space (before or after penetrating the satellite shielding) or to the spectrum of secondary electrons produced by γ-rays. One has just to average NIEL(T_0) of Eq. (2) (or of the plots in Fig. 1) over the electron spectrum using the electron energy distribution normalized to one electron or one photon.

[1] www.research.ibm.com/ionbeams/SRIM/SRIMLEGL.HTM

5. NIEL for γ-rays

The γ-rays from a ^{60}Co source (with γ-rays of energy $E_\gamma = 1.25$ MeV) are used as an irradiation standard. For $E_\gamma > 0.511$ MeV, the main process of the interaction of γ's with matter is the Compton scattering. (At very high energies it is the electron–positron pair production.) The differential cross section $d\sigma/dT$, for an energy-transfer T to a free electron in a solid of atomic number Z, is given by Heitler (1944)

$$d\sigma/dT = (\pi r_0^2 m_0 c^2 Z/E_\gamma^2)\{2 - 2T/[\alpha(E_\gamma - T)] + T^2[E_\gamma + \alpha^2(E_\gamma - T)]/[\alpha^2(E_\gamma - T)^2 E_\gamma]\}, \quad (10)$$

where r_0 is the classical electron radius, $m_0c^2 = 0.511$ MeV is the electron rest energy, E_γ is given in MeV and $\alpha = E_\gamma/0.511$ MeV. Eq. (10) gives the initial spectrum of the Compton electrons. It is good for $E_\gamma > 0.1$ MeV for which we can omit the form-factor added at lower energies to account for the electron binding.

During their transport through matter Compton electrons lose energy. At any given point the spectrum of these electrons should be calculated by adding the contributions of all electrons reaching this point from Compton scattering events in its surroundings. In order to calculate the NIEL parameter at the given point in the material (Si or GaAs) we have to integrate this spectrum distribution (per incident photon) with the appropriate NIEL values plotted in Fig. 1. The surroundings include the device materials (silicon or GaAs, aluminum, ceramics, glass, etc.) and shielding materials (aluminum, lead).

For simplicity we take the surrounding as an equivalent aluminum shielding with given thicknesses. To calculate the spectra of the Compton electrons we have used our Monte Carlo code based on the algorithms described by Akkerman et al. (1986). We take a unidirectional beam of γ-rays from ^{60}Co and calculate the energies of the electrons created in the aluminum plate and exiting it in the forward (half hemisphere) direction. Fig. 2 shows our calculated secondary electron spectra per γ photon in the case of a shielding with a thickness of 100, 500, 1000, 1500, and 2000 μm. As is obvious from the figures, the spectra converge to an equilibrium spectrum for thicknesses larger than 1500 μm. Our calculated spectra differ significantly from those presented by Summers et al. (1993). We have no explanation for this difference. Our Monte Carlo code was checked by calculating the transmission curve and backscattering spectra for electrons of different energies, and by comparing them with the experimental data cited by Akkerman et al. (1986). A close agreement has been found.

In Fig. 3 we present our calculated γ-rays NIEL (per one photon) for silicon and GaAs as a function of the shielding thickness. The maximum in the NIEL is due to the saturation in the secondary electron spectra shown in Fig. 2.

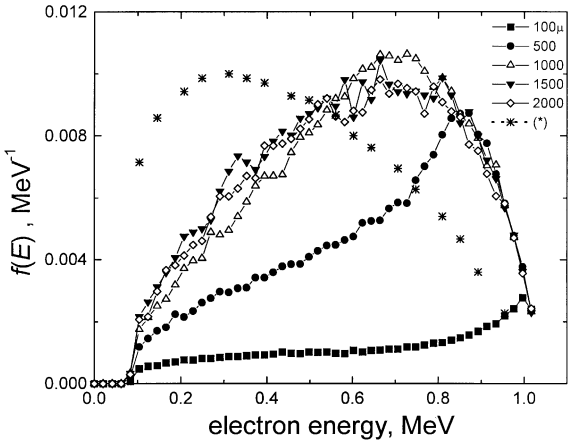

Fig. 2. The spectra of electrons emitted by ^{60}Co after passing shieldings of thicknesses from 100 μm to 2 mm. Note the difference with the equilibrium spectrum of Summers et al. (1993) marked by symbols.

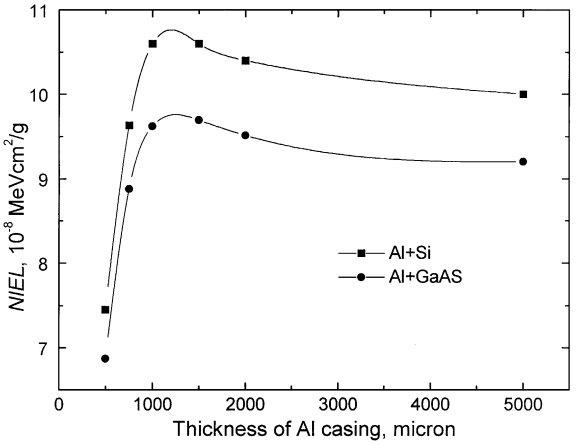

Fig. 3. The ^{60}Co γ-ray NIEL in Si and GaAs as function of the Al shielding thickness.

Fig. 3 shows that, up to 1 mm, NIEL increases as a function of the thickness. For GaAs the NIEL values are systematically lower than for Si although the threshold displacement energy T_{min} for GaAs is half that of Si. This is the result of lower recoil energies of the GaAs atoms as compared with those of the Si atoms.

Since the ^{60}Co source is well shielded in usual γ-cells, it can be assumed that in actual experiments the NIEL reaches its equilibrium value shown at the right hand side of Fig. 3. For aluminum shielding the equilibrium

value (per one photon) is

$$\mathrm{NIEL}_\gamma(\mathrm{Si}) = 1.07\times10^{-7}\ \mathrm{MeV\,cm^2/g} \quad \text{and}$$
$$\mathrm{NIEL}_\gamma(\mathrm{GaAs}) = 9.7\times10^{-8}\ \mathrm{MeV\,cm^2/g}.$$

6. NIEL for protons

Two processes of proton interaction in matter are responsible for creating recoils which introduce displacement damages: (1) *elastic scattering* with cross section σ_{elas}, (2) *inelastic scattering* (nuclear reactions) with cross section σ_{inel}. Examination of the relative importance of these processes, $(\sigma_{\mathrm{elas}}/\sigma_{\mathrm{inel}})$ versus proton energy has shown that below 30 MeV the role of the inelastic scattering in the damaging process might be assumed negligible. When the proton energy increases the role of the inelastic interaction becomes the dominant process (Barak et al., 1999). The recoils have larger energies which might even change the character of the created damages. The change is related to the development of separated cascades of displacements with reduced recombination rates.

6.1. Elastic scattering

Protons are subjected to Coulomb repulsion from the nucleus charge. Quantitatively, this interaction is described by the differential non-relativistic Rutherford cross section $(\mathrm{d}\sigma/\mathrm{d}\Omega)_{\mathrm{R}}$ given by

$$(\mathrm{d}\sigma/\mathrm{d}\Omega)_{\mathrm{R}} = \frac{e^4Z^2}{4T_0^2(1-\cos\theta)^2}, \tag{11}$$

where $e^2 = 1.44\times10^{-13}$ MeV cm is the square of the elementary charge, Z is the target atomic number, $T_0(=E_{\mathrm{p}})$ is the proton kinetic energy in MeV and θ is the CM scattering angle. Besides the Coulomb interaction, the proton (as a nuclear particle) experiences interaction with the nuclear field. This kind of interaction shows a distinct behavior of a sequence of diffraction peaks in the angular distribution of the scattered protons. This is treated in the frame of the optical model (Lafond, 1969). For a comparison of our results with the experimental data, which are almost always presented as $(\mathrm{d}\sigma/\mathrm{d}\Omega)/(\mathrm{d}\sigma/\mathrm{d}\Omega)_{\mathrm{R}}$, we scale our data to $(\mathrm{d}\sigma/\mathrm{d}\Omega)_{\mathrm{R}}$ (by matching the values at small angles). We found that the calculated $\mathrm{d}\sigma/\mathrm{d}\Omega$ values of the ENDF/B-VI library are, in general, in a very close agreement with the existing experimental data. This supports the use of the theoretical (ENDF/B-VI) $\mathrm{d}\sigma/\mathrm{d}\Omega$ for systematic NIEL calculations. In order to use expression (2) we first approximate the $\mathrm{d}\sigma/\mathrm{d}\Omega$ data, tabulated in ENDF/B-IV, by a sum of a few Gaussians. The energy transferred to the recoil is calculated using Eq. (3).

6.2. Inelastic scattering

This process stands for a variety of nuclear interactions, starting from the excitation of nuclear levels [(p, p′) reactions] to more complicated ones which are followed by emitting light particles and creating energetic recoils (Akkerman et al., 1996). The ENDF/B-VI data used in the present work were based on well established nuclear reaction theories that are suitable for application up to approximately 200 MeV (Hodgson and Godioli, 1992; Chadwick et al., 1999b). Direct, pre-equilibrium, and Hauser–Feshbach compound nucleus reaction mechanisms are included. In the early stages of the reaction, one or more high energy light pre-equilibrium ejectiles can be emitted, leaving a residual nucleus in an excited state. This then decays by sequential compound nucleus particle and/or γ-ray emission, until a final residual nucleus is produced in its ground or isomeric state. At each stage of the reactions, the kinematics of the nucleus is tracked so that the final recoiling kinetic energy of the reaction products are known. Thus, the ENDF/B-VI library contains the recoil spectra for different reaction channels. These data might be used directly in Eq. (1).

We have used the ENDF/B-VI data for proton energies $E_{\mathrm{p}} < 150$ MeV and our semi-empirical model (Akkerman et al., 1996) for $E_{\mathrm{p}} > 150$ MeV, to calculate the energy distribution of the recoils. In order to show that this is a good extension to the ENDF/B-VI data we compare in Table 1 (for $E_{\mathrm{p}} = 100$ and 150 MeV) the relative distribution of the partial fragmentation cross sections estimated using ENDF/B-VI with the results of our model. The agreement is quite good except for the group of recoils with atomic numbers between $Z = 8$ and 11. However, the differences are too small to cause significant differences in the NIEL values.

6.3. Proton induced NIEL in silicon

Fig. 4 shows the results of the calculated NIEL versus proton energy E_{p} due to proton interactions in Si for (i) the elastic scattering, using the optical model, (ii) the inelastic scattering, and (iii) their sum (total). They are compared with the total NIEL calculated by Summers et al. (1993). Below $E_{\mathrm{p}} = 60$ MeV our results are very close to those of Summers et al. (1993). At higher energies our NIEL values are smaller. Since at these energies the major contribution to NIEL comes from inelastic scattering, it is believed that this difference is due to the use of different models for inelastic proton interaction. To demonstrate the changes from an often used model (HETC) to ENDF/B-VI, we show in Table 2 the partial cross sections for creating (in silicon) the main recoiling atoms, along with their mean energies, for $E_{\mathrm{p}} = 70$ and 100 MeV. Our calculated data, using the ENDF/B-VI, are compared with those calculated by

Alurralde et al. (1991). One might see that the major deviation (both in the cross sections and the mean recoil energy) appears for the group of the most damaging recoils: Si, Al and Mg. Such differences might give rise to the deviations observed in Fig. 4.

Fig. 4 shows that if we know the proton induced NIEL for one energy, we have the theoretical means to scale it to other energies or to the distribution of energies in space. In Section 7 we will discuss the use of Figs. 4 and 5 for this purpose.

6.4. Proton induced NIEL in GaAs

As there are no data in the ENDF/B-VI library for Ga with $Z = 31$ or for As with $Z = 33$ we used the data for Cu with $Z = 29$ (the closest one available in ENDF/B-

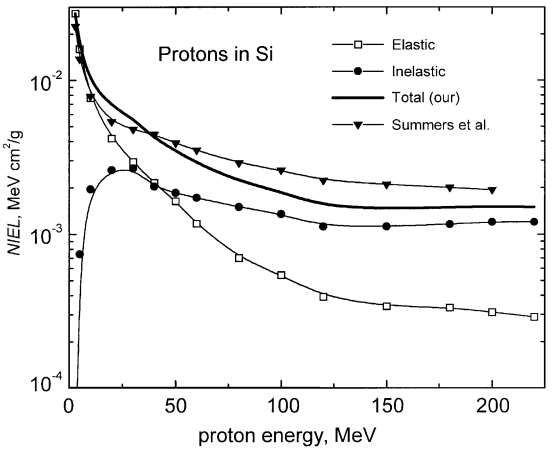

Fig. 4. Our calculated values of NIEL in Si versus proton energy for the different channels of interactions, compared with the results of Summers et al. (1993).

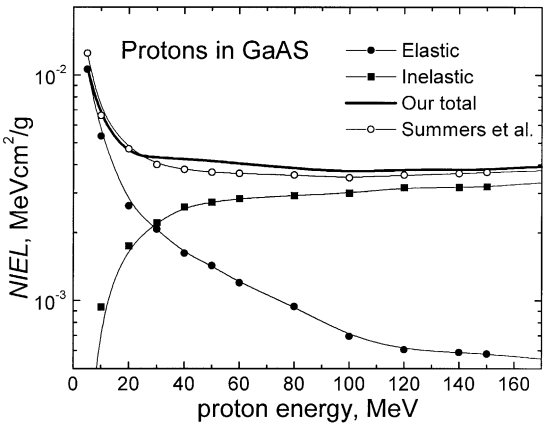

Fig. 5. Our calculated values of NIEL in GaAs versus proton energy for the different channels of interactions, compared with the results of Summers et al. (1993).

Table 2
Proton nuclear reactions in silicon: comparison of the partial cross sections σ and mean recoil energy E_m, calculated by two codes, HETC (Alurralde et al., 1991) and ENDF/B-VI (present work), for 70 and 100 MeV protons

Recoil	HETC partial σ (mb)	ENDF/B-VI partial σ (mb)	HETC E_m (MeV)	ENDF/B-VI E_m (MeV)
$E_p = 70$ MeV				
Si	163 ± 8	110	0.46 ± 0.03	1.6
Al	144 ± 8	148	0.99 ± 0.07	2.1
Mg	166 ± 8	144	1.77 ± 0.1	2.3
Na	31 ± 3	47	2.8 ± 0.4	2.7
Ne	27 ± 3	25	3.1 ± 0.5	3.0
F	—	3	—	3.4
O	7 ± 2	5	3.1 ± 1	3.8
He	133 ± 7	125	6.7 ± 0.5	8.6
$E_p = 100$ MeV				
Si	123 ± 4	75	0.47 ± 0.02	1.2
Al	123 ± 4	113	0.9 ± 0.07	2.3
Mg	121 ± 4	107	1.7 ± 0.07	2.6
Na	41 ± 2	48	2.9 ± 0.2	2.9
Ne	44 ± 2	45	3.1 ± 0.2	3.2
F	—	14	—	3.8
O	17 ± 1	9	4 ± 0.4	4.1
N	—	6	—	4.1
C	—	2	—	4.9
He	154 ± 4	144	6.8 ± 0.2	9.1

VI) to calculate the NIEL for elastic and inelastic proton interactions in GaAs.

For the elastic scattering the ENDF/B-VI data for protons in copper have been scaled according to Z and A for Ge ($Z = 32$) in order to be used for GaAs. That this is a good scaling for different nuclei had been proved in the comparison between the experimental elastic scattering data for Cu, Zn and Sr (Becchetti and Greenlees, 1969). Thus, when using this scaling method, only small deviations are expected in the calculation of $d\sigma/d\Omega$ and of NIEL values.

For inelastic proton scattering we have found that the above approach yields total inelastic cross sections which are not more than 10% below the phenomenological systematics-based results given by Wellisch and Axen (1996). Also, the ENDF/B-VI partial cross section for Cu are in good agreement with the often used data of Petersen (1980). We thus use for our GaAs 'inelastic' calculations these unchanged partial cross sections of Cu and for the 'elastic' calculations the above scaling procedure. As can be seen in Fig. 5, the agreement with the NIEL of Summers et al. (1993) is very good for protons in GaAs.

6.5. NIEL for neutrons

It has been shown, long ago, that at energies $E > 20$ MeV neutrons and protons with the same energy behave in matter in similar ways both in the elastic and inelastic scattering (Petersen, 1980). This means that neutrons-NIEL should be close to that for protons. Differences are expected at lower energies due to the Coulomb barrier. Experimental difficulties prevent the creation of beams of energetic neutrons in accelerators, except for the 14 MeV neutrons obtained in d-t neutron generators. One of the most useful sources of neutrons are nuclear reactors with fission neutrons. Here, it is assumed that the fission spectrum simulates well the displacement damage due to 1 MeV neutrons. This is the reason why in many procedures the estimation of the displacement damage of a given fluence of particles is done by finding the 'equivalent fluence' of 1 MeV neutrons which would give rise to the same damage. For this purpose we have estimated the NIEL factor of 1 MeV neutrons scattered in silicon and GaAs (calculated for germanium). They are given by

$$\mathrm{NIEL_n(Si)} = 2.04\times10^{-3}\ \mathrm{MeV\,cm^2/g} \quad \text{and}$$
$$\mathrm{NIEL_n(GaAs)} = 5.3\times10^{-4}\ \mathrm{MeV\,cm^2/g}.$$

These values are in agreement with those cited in the literature.

7. Damage and equivalent fluence estimations

7.1. The displacement damage factor

Having calculated the NIEL for different particles and energies we need to know to what extent the estimated NIEL is a good measure of the displacement damage introduced in real electronic devices. The damage is usually characterized by the damage factor K_i which relates the given degraded characteristic (i stands for mobility, resistance, minority carrier life-time, diffusion length, etc.) to the fluence of particles Φ ($\mathrm{cm^{-2}}$), according to the relation

$$Y_i/Y_{i0} = (1 + K_i\Phi), \tag{12}$$

where Y_{i0} and Y_i are the values of the given characteristic of the device before and after irradiation, respectively. For resistivity measurements $Y_i = R$, for mobility measurements $Y_i = 1/\mu$, and for the degradation of the minority carriers life-time L, $Y_i = 1/L^2$.

Many experimental investigations have shown that to first order (for each particle separately) one might assume a linear proportionality, independent of the particle, between the damage factor K_i and the particle NIEL (for references see Marshall and Marshall, 1999). This is the essence of the use of the NIEL parameter since it allows to measure K_i only for one particle (at one specified energy) from which the K_i values for all particles (and energies) are easily estimated.

The simplest case is when K_i^{a} is measured for one proton energy $E_{\mathrm{p}}^{\mathrm{a}}$. Then we find it for any other energy $E_{\mathrm{p}}^{\mathrm{b}}$ by $K_i^{\mathrm{b}} = K_i^{\mathrm{a}}\,\mathrm{NIEL}(E_{\mathrm{p}}^{\mathrm{b}})/\mathrm{NIEL}(E_{\mathrm{p}}^{\mathrm{a}})$ using the values in Figs. 4 or 5. As an example of using different particles we take protons (p) and neutrons (n). Then for any damage factor K

$$K_{\mathrm{p}}/K_{\mathrm{n}} = \mathrm{NIEL_p/NIEL_n}. \tag{13}$$

Here we consider K_{n} for 1 MeV neutrons. Fig. 6 depicts the results of our calculations of the damage factor ratio $K_{\mathrm{p}}/K_{\mathrm{n}}$ versus proton energy E_{p} in Si and GaAs. The sharp drop of $K_{\mathrm{p}}/K_{\mathrm{n}}$ for $E_{\mathrm{p}} > 60$ MeV was confirmed experimentally by Pease et al. (1987) whereas the data of Summers et al. (1993) do not show such a behavior.

Very seldom damage measurements would be performed using fission neutrons. More often data are collected using protons or electrons (less frequently using γ-rays). To convert the damage factor ratios of Fig. 6 ($K_{\mathrm{p}}/K_{\mathrm{n}}$) to the corresponding ratios of electrons ($K_{\mathrm{p}}/K_{\mathrm{e}}$) or for 1.25 MeV γ-rays of ^{60}Co ($K_{\mathrm{p}}/K_{\gamma}$), one has to multiply the values in Fig. 6 by the ratios $\mathrm{NIEL_n/NIEL_e}$ or $\mathrm{NIEL_n/NIEL_\gamma}$. These values are given in Table 3 for ^{60}Co and electron energies of 1 and 10 MeV. They were calculated by dividing the above $\mathrm{NIEL_n}$ values (for Si and GaAs) by the appropriate $\mathrm{NIEL_e}$

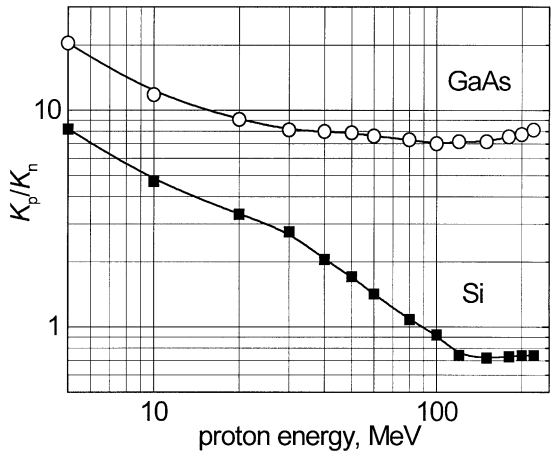

Fig. 6. The relative damage, K_p/K_n, as a function of proton energy where K_n is taken for 1 MeV neutrons.

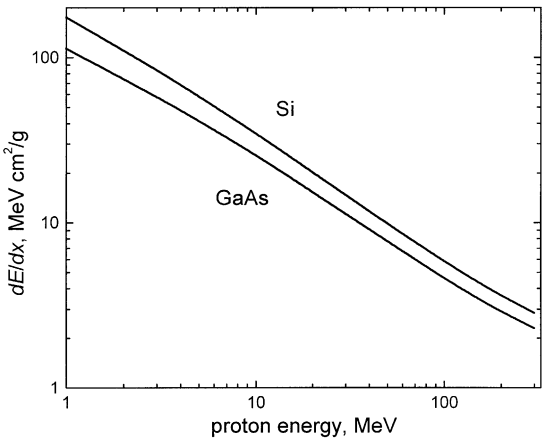

Fig. 7. The stopping power dE/dx of protons in silicon and GaAs as a function of proton energy, calculated using SRIM-2000.

Table 3
The scaling factors to estimate the damage factor ratios K_p/K_e or K_p/K_γ (for electrons and ^{60}Co γ-rays respectively) from K_p/K_n of Fig. 6

Material	Electrons		^{60}Co γ-rays
	1 MeV	10 MeV	1.25 MeV
Si	63.6	18.7	1.92×10^4
GaAs	22	6.2	5.5×10^3

values from Fig. 1 and the equilibrium values of $NIEL_\gamma$ from Fig. 3.

7.2. The equivalent fluence factor

To estimate the changes in a given characteristic Y after a certain particle irradiation, using Eq. (12), we need to know the fluence Φ of this particle. For an ionizing particle Φ is proportional to the absorbed dose D to a material (Si or GaAs) through the expression

$$D[\mathrm{Gy}] = 1.6\times10^{-10}\,\mathrm{d}E/\mathrm{d}x\,(\mathrm{MeV\,cm^2/g})\Phi, \quad (14)$$

where $\mathrm{d}E/\mathrm{d}x$ in MeV cm^2/g is the LET value of protons as given in Fig. 7 which is calculated using SRIM-2000 (Ziegler et al., 1985). We checked that the maximal difference between the stopping powers of SRIM and those of ICRU-49 Report (ICRU, 1993) is 2% for Si and 3% for GaAs. Eqs. (13) and (14) give a convenient way to estimate Φ when (like in ^{60}Co irradiation) the dose D cannot be measured by counting particles with a detector.

Alternatively we can follow the 'equivalent neutron fluence Φ_n' approach suggested by Raymond and Petersen (1987). For protons it yields the expression

$$\Phi_n = R_p D, \quad (15)$$

where R_p can be calculated using the relative damage factor K_p/K_n plotted in Fig. 6,

$$R_p = (K_p/K_n)/(D_p/\Phi_p), \quad (16)$$

with D_p/Φ_p calculated using Eq. (14).

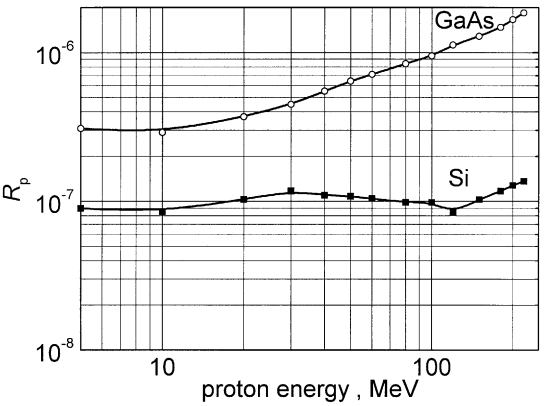

Fig. 8. The proton–neutron equivalence factor R_p for Si and GaAs versus proton energy.

The equivalence factor R_p is shown in Fig. 8 as a function of proton energy. R_p for Si is practically independent of proton energy. This is due to the fact that R_p is proportional to the ratio of $NIEL_p$ and LET_p which have a similar dependence on E_p (Raymond and Petersen, 1987). For GaAs, the equivalent neutron fluence (for the same absorbed dose) remains practically the same for proton energies up to 20 MeV above which the equivalent fluence increases. Such a behavior is due

to the partition of the recoil energy loss to ionization and damage.

In space, we deal with spectra of particles (e.g. protons) with spectral distribution of fluence $\Phi(E)$ and the corresponding NIEL(E) values. In this case the equivalent fluence for testing with monoenergetic particles with energy E_1 (and one value $NIEL_1$) is found by integrating NIEL(E) with the differential fluence $d\Phi/dE$, over the energy E. The equivalent fluence of the monoenergetic particles is obtained by dividing the result of integration by $NIEL_1$ (Marshall and Marshall, 1999). All the needed data are presented above.

8. Discussions

We believe that the present results are useful for assessing the use of devices, sensitive to displacement damage, for space missions. Yet, we have to keep in mind that the NIEL results are related only to the first stage of damage processes by the recoils which cannot be detected. Through processes, which are not yet well understood, simple defects like vacancy-interstitial (Frenkel) pairs are transformed to stable defects like complexes of vacancies or of vacancies and impurity atoms. These defects and their influence on the device parameters can be detected. It is thus difficult to assume that the calculated NIEL which estimate the damage of the first stage is also a good measure of the real defects of the final stage of the damaging process. Only if there is a proportionality between the damage factor K and the corresponding NIEL (like $K_p \propto NIEL_p$), one can expect the NIEL to be a real measure of radiation defects in devices. In a part of the experiments this linearity was shown and in-orbit quantitative estimations have been done (Marshall and Marshall, 1999). On the other side it was shown by Dale et al. (1989b) that for transistors made from n-Si and p-Si as well as for several Charge Injection Devices and CCDs there is a deviation from proportionality. Similar deviations for oxygen- and carbon-enriched Surface Barrier Detectors, used in high energy experiments in CERN, have been reported by Ruzin et al. (1999). It was proposed that this deviation should be related to the structure of the cascading process of the primary recoil spectrum and the recombination rate of Frenkel pairs in the damaged region. In several cases, the estimation of the recombination rates, needed to explain the deviations, are in contradiction with a computer simulation of the evolution of the damage region. Hence, the NIEL concept has to be used with care. Laboratory damage measurements for one or more proton energies, when added to the NIEL calculations, will ensure the satellite designers of the reliability of the device functioning in space.

9. Summary

We have presented new calculations of NIEL in a wide range of energies for particles and γ-rays in Si and GaAs using the models and expressions we believe are the most appropriate for this task. In general, our results are in a good agreement with previous calculations and thus verify them and update them to a better precision. In particular, the new ENDF/B-VI data base has been used for the spectra of recoils of elastic and inelastic scattering of protons and neutrons in Si and GaAs. The ENDF/B-VI data were calculated to 150 MeV and were extended here to above 200 MeV using our semi-empirical model which is compatible with HETC calculations.

The calculated results are presented in a form useful for damage estimation in space as well as for planning laboratory experiments and calculating the equivalent particle fluences when performing laboratory tests. Some limitations in using the NIEL concept have been discussed.

Acknowledgements

We are indebted to Eugene Normand for useful discussions.

References

Akkerman, A.F., 1991. Modeling of Charged Particle Trajectories in Matter. Energoatomizdat, Moscow, 200p (in Russian).

Akkerman, A., Barak, J., Levinson, J., Lifshitz, Y., 1996. Modeling of proton induced SEUs. Radiat. Phys. Chem. 48, 11–22.

Akkerman, A.F., Grudskii, M.Ya., Smirnov, V.V., 1986. Secondary Electron Radiation from Solids Induced by γ-rays. Energoatomizdat, Moscow, 166p (in Russian).

Alurralde, M., Victoria, M., Caro, A., Gavillet, D., 1991. Nuclear and damage effects in Si produced by irradiations with medium energy protons. IEEE Trans. Nucl. Sci. 38, 1210–1215.

Barak, J., Levinson, L., Akkerman, A., Adler, E., Zentner, A., David, D., Lifshitz, Y., Hass, M., Fisher, B.E., Schlögl, M., Victoria, M., Hadjas, W., 1999. Scaling of SEU mapping and cross section, and proton induced SEU at reduced supply voltage. IEEE Trans. Nucl. Sci. 46, 1342–1353.

Becchetti Jr., F.D., Greenlees, G.W., 1969. Nucleon-nucleus optical-model parameters, $A > 40$, $E < 50$ MeV. Phys. Rev. 182, 1190–1209.

Berger, M.J., Seltzer, S.M., Wang, R., Schechter, A., 1993. Elastic scattering of electrons and positrons by atoms: database ELAST, NISTR 5188, Washington, DC 20585.

Bunyan, P.J., Schonfelder, J.L., 1965. Polarization by mercury of 100 to 2000 eV electrons. Proc. Phys. Soc. 85 (545), 455–462.

Chadwick, M.B., Normand, E., 1999. Use of new ENDF/B-VI proton and neutron cross section for single event upset calculations. IEEE Trans. Nucl. Sci. 46, 1386–1394.

Chadwick, M.B., Young, P.G., Chiba, S., Frankle, S.C., Hale, G.M., Huges, H.G., Koning, A.J., Little, R.C., MacFarlane, R.E., Prael, R.E., Waters, L.S., 1999b. Cross sections evaluation to 150 MeV for accelerator-driven system and implementation in MCNPX. Nucl. Sci. Eng. 131, 293–328.

Chadwick, M.B., Young, P.G., MacFarlane, R.E., Moller, P., Hale, G.M., Little, R.C., Koning, A.J., Chiba, S., 1999a. LA150 documentation of cross sections, heating, and damage: Part A (incident neutrons) and Part B (incident protons), Los Alamos National Laboratory report LA-UR-99-1222 (available on the Web at http://t2.lanl.gov/publications/la150/la150.html). See also IRCU Report 63. (2000) Nuclear Data for Neutron and Proton Radiotherapy and for Radiation Protection. International Commission on Radiation Units and Measurements, Bethesda, MD.

Dale, C.J., Marshall, P.W., Burke, E.A., Summers, G.P., Bender, G.E., 1989b. The generation lifetime damage constant and its variance. IEEE Trans. Nucl. Sci. 36, 1872–1881.

Dale, C.J., Marshall, P.W., Summers, G.P., Wolicki, E.A., Burke, E.A., 1989a. Displacement damage equivalent to dose in silicon devices. Appl. Phys. Lett. 54, 451–453.

Heitler, W., 1944. The Quantum Theory of Radiation. Oxford University Press, London.

Hodgson, P.W., Gadioli, E., 1992. Pre-Equilibrium Nuclear Reactions. Oxford Studies in Nuclear Physics Series. Clarendon Press, Oxford.

ICRU-49 Report, 1993. Stopping Powers and Ranges for Protons and Alpha Particles, International Commission on Radiation Units and Measurements, Bethesda, MD.

Lafond, G. de, 1969. Interactions proton silicium et proton germanium entre 1 et 3000 MeV. Thèse d'état, université Paul Sabatier, Toulouse.

Lijian, J., Qing, H., Zhengming, L., 1995. Analytic fitting to the Mott cross section of electrons. Rad. Phys. Chem. 45, 235–245.

Lindhard, J., Nielsen, V., Scharf, M., Thomsen, P.V., 1963. Mat. Fys. Medd. Dan. Vid. Selsk. 33 (10).

Marshall, C.J., Marshall, P.W., 1999. Proton effects and test issues for satellite designers, part B: displacement effects. IEEE NSREC Short Course, July 12, 1999, IV50–IV110.

Messenger, S.R., Burke, E.A., Summers, G.P., Xapsos, M.A., Walters, R.J., Jackson, E.M., Weaver, B.D., 1999. Non-ionizing Energy Loss (NIEL) for Heavy Ions. IEEE Trans. Nucl. Sci. 46, 1595–1602.

Mott, N.F., Massey, H.S.W., 1965. The Theory of Atomic Collisions, 3rd Edition . Clarendon Press, Oxford ((Chapter 8)).

Motz, J.W., Olsen, H., Koch, H.W., 1964. Electron scattering without atomic or nuclear excitation. Rev. Mod. Phys. 36, 881–928.

Nigam, B.P., Sundaresan, M.K., Wu, T.-Y., 1959. Theory of multiple scattering: second born approximation and corrections to Molière's work. Phys. Rev. 115, 491–502.

O'Connor, D.J., Biersack, J.P., 1986. Comparison of theoretical and empirical interatomic potentials. Nucl. Instrum. Meth. B 15, 14–19.

Pease, R.L., Enlow, E.W., Dinger, G.L., Marshall, P., 1987. Comparison of proton and neutron carrier removal rates. IEEE Trans. Nucl. Sci. 34, 1140–1146.

Petersen, E.L., 1980. Nuclear reactions in semiconductors. IEEE Trans. Nucl. Sci. 27, 1494–1500.

Raymond, J.P., Petersen, E.L., 1987. Comparison of neutron, proton and γ-ray effects in semiconductor devices. IEEE Trans. Nucl. Sci. 34, 1622–1628.

Robinson, M.T., 1968. The influence of the scattering law on the radiation damage displacement cascade. II. Phil. Mag. 17, 639–642.

Ruzin, A., Casse, G., Glaser, M., Zanet, A., Lemeilleur, F., Watts, S., 1999. Comparison of radiation damage in silicon induced by proton and neutron irradiation. IEEE Trans. Nucl. Sci. 46, 1310–1313.

Summers, G.P., Burke, E.A., Shapiro, P., Messenger, S.R., Walters, R.J., 1993. Damage correlations in semiconductors exposed to γ, electron and proton radiations. IEEE Trans. Nucl. Sci. 40, 1372–1379.

Wellisch, H.P., Axen, D., 1996. Total reaction cross section calculations in proton-nucleus scattering. Phys. Rev. C 54, 1329–1332.

Ziegler, J.F., Biersack, J.P., Littmark, U., 1985. The Stopping and Range of Ions in Solids. Pergamon Press, New York.